

Coupled Electro-thermal Field Simulation in HVDC-Cables

Hanyu Ye¹, El Mehdi Boudoudou¹, Eike Scholz¹ and Markus Clemens¹
¹Chair of Electromagnetic Theory, Bergische Universität Wuppertal, Germany

Abstract: Electric field distributions for high-voltage direct current cables (HVDC-cables) are usually modeled as electrostatic problems under the assumption that the material properties are linear. In this paper the nonlinear properties of the insulator material polyethylene and the ohmic losses in the insulation material are taken into account. Results for coupled electro-thermal simulations for a rotationally symmetric and a non-rotationally symmetric model are presented.

Keywords: coupled electro-thermal field simulations, PE Cables

1. Introduction

Compared to other conventional cables such as oil-paper or mass-impregnated cables, PE (Polyethylene) insulated cables have some advantages: light weight, almost maintenance free, simple chemical assembly and good electric-thermal properties. Thus it has commercial and technical advantages to use PE as the insulation material for the HVDC-cables, especially for long-distance power transmission. The electric field distribution in the insulation depends on the conductivity κ of the insulation material which is affected by the temperature and the electric field strength. However most simulations for HVDC-cables are performed as electrostatic problems under the assumption that the material properties are linear and the thermal effects are neglected as well.

A coupled electro-thermal one dimensional model of a rotationally symmetric HVDC-model-cable is presented in [1], taking the nonlinear properties of the insulator material into account. But in that publication the ohmic losses in the insulation are neglected, because the conductivity κ is always very low in the PE insulation compared to κ in copper conductor [2]. In this paper the ohmic losses in the insulation are also considered and the results are compared to the results in [3]. Furthermore an extended two-dimensional model for the coupled electro-thermal simulation of HVDC-cables is implemented

using COMSOL Multiphysics. This enables us to simulate cables without rotational symmetry in the cross-section. Additionally the mutual dependence between temperature and electric field strength for both a stationary and a time-dependent model is examined based on the nonlinear weak coupling of the specific direct current conductivity κ with the electric field strength and the temperature.

2. Problem Modeling

In this section the material properties of PE and the mathematical formulation for this problem are introduced.

2.1 Material Properties

The insulation material PE is nonlinear and has a low electric conductivity κ , which is affected by temperature and field strength. The specific direct current conductivity κ can be approximated by the following function, which is often used in the related literature [4, 5, 6]:

$$\kappa(\vartheta, |\vec{E}|) = k_0 \cdot \exp(\alpha \cdot \vartheta) \cdot \exp(\beta \cdot |\vec{E}|) \quad (1)$$

k_0	specific direct current conductivity at 0°C and 0kV/mm
ϑ	temperature in °C
$ \vec{E} $	electric field in kV/mm
α	temperature coefficient of the specific direct current conductivity
β	field strength coefficient of the specific direct current conductivity

The typical values for Polyethylene are [2]:

$$\alpha \approx 0,1K^{-1}$$
$$\beta \approx 0.1mm/kV$$

Standard values for other polymeric isolation materials are given in [7]. The PE-Compounds can be significantly distinguished by the absolute specific conductivity k_0 . A comparison of the coefficients for some different types of PE-Compounds is given in table 1.

Material	k_0 [S/mm]	α [1/°C]	β [mm/kV]
VPE Type A	$15,1 \cdot 10^{-19}$	0,086	0,137
MDPE Type B	$0,297 \cdot 10^{-19}$	0,094	0,121
VPE Type B	$0,259 \cdot 10^{-19}$	0,108	0,115

Table 1: Parameters of the specific conductivity for the different PEs [3].

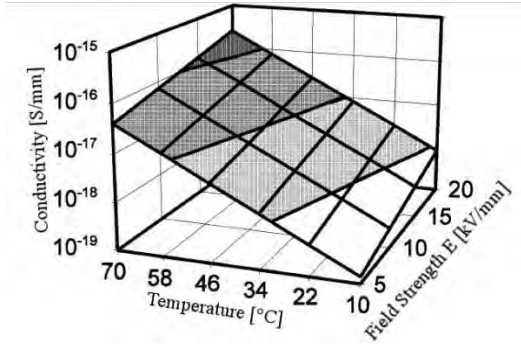


Fig. 1: An approximated function for the specific direct current conductivity for MDPE Type B [3]

The field- and temperature-dependent conductivity κ of the insulation material MDPE Type B, which is mathematically approximated via eqn. 1, can be found in Fig. 1.

It should be noted that the heat conductivity of PE depends on the temperature. For the cable MDPE type B the thermal conductivity can be approximated as:

$$\lambda = (0,72 - 0,001 \cdot T), \quad (2)$$

where T is the absolute temperature in K and this formula is valid just for $10^\circ\text{C} \leq \vartheta \leq 90^\circ\text{C}$ [3].

2.2 Mathematical Formulation

The electric field distribution is mathematically described by partial differential equations, which are derived from the continuity equation:

$$\text{div} \vec{J} + \partial_t \rho = 0. \quad (3)$$

For HVDC-cables the term $\partial_t \rho$ can be omitted because the applied voltage is constant. With ohm's law $\vec{J} = k \cdot \vec{E}$ and $\vec{E} = -\text{grad} \varphi$, where $k = k(\vartheta, \vec{E})$, eqn. 3 can be transformed to:

$$\text{div}(k(T, \varphi) \cdot \text{grad} \varphi) = 0, \quad (4)$$

where T is the temperature in K , φ is the scalar potential and $k(T, \varphi)$ is the approximated material property function (Eqn. 1).

The temperature distribution in the insulation material is described by the heat conduction equation, which is derived from Fourier' law and the law of energy conservation [8]:

$$C_p \cdot \rho \cdot \partial_t T - \text{div} \lambda \cdot \text{grad} T = Q_E + Q_M \quad (5)$$

where C_p is the heat capacity at constant pressure, ρ is the density, λ is the thermal conductivity, Q_E describes electric heat sources and Q_M describes mechanic heat sources. For this application Q_M can be neglected and Q_E consists of two parts: joule heating from the cable Q_C and ohmic losses from Q_I in the insulation material with:

$$Q_I = k(T, \varphi) \cdot (\text{grad} \varphi)^2. \quad (6)$$

Thus the eqn. 5 can be written as:

$$C_p \cdot \rho \cdot \partial_t T - \text{div} \lambda \cdot \text{grad} T = Q_C + Q_I. \quad (7)$$

Now the eqn. 3 and eqn. 7 can be weakly coupled by the material property eqn. 1. They can be solved numerically using the FEM (Finite Element Method) software COMSOL Multiphysics, if the geometry and the boundary conditions are given. For this paper they are discretized in space using FEM with higher order elements. Time integration is done by a suitable time integrator [9].

For the stationary situation the heat conduction equation can be formulated as:

$$-\text{div} \lambda \cdot \text{grad} T = Q_C + Q_I, \quad (8)$$

under the assumption that the inflowing heat to the inspected domain is equal to the outflowing heat from this domain.

3. Numerical Results

The simulations are realized using the in COMSOL integrated Joule Heating model. Different simulations are carried out to examine the influence of the temperature on the distribution of the electric field for stationary and time-dependent cases. For the stationary case, the influence of the temperature difference ΔT across the insulation material and the coefficient β for the material function is investigated. Additionally the simulation results for a non-rotationally symmetric model are presented.

3.1 Simulation Model

To compare the simulation results with the results in [3], a simplified small two-dimensional sample model of a real power cable insulation is used (Fig. 2). The copper conductor can be seen as a cylinder and its potential is set to 200kV. To simplify the problem, the conductor has been cut out of the model and replaced with an equivalent boundary condition. The outside field shielding is set to 0kV. The simulation results are evaluated along an evaluation line which is shown in Fig. 3.

3.2 Stationary Study

In this study the simulations are carried out under the assumption that the surface temperature of the inside conductor is constant at 90°C, because the experiments in [3] are realized with this temperature. The non-linearity of PE insulation material, especially the dependence on the temperature, has the following consequence: The temperature difference ΔT between the inside conductor and the outside field shielding has a significant influence on the electric field distribution in the insulation material [2, 10, 11]. Fig. 4 and Fig. 5 show the temperature and electric field distributions in the insulation material. Normally the electrostatic field strength is higher at the inner radius than at the outer one. From Fig. 5 we can see that the electric field strength decreases at the inside radius and increases at the outside radius if the temperature difference ΔT increases. This effect is called inversion of field strength [12]. Additionally the influence of the electric field coefficient β with a constant ΔT for the field distribution is shown in Fig. 6. For increasing

values of β , the electric field strength at the outside field shielding decreases.

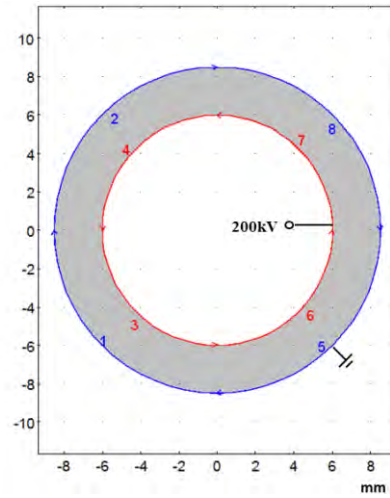


Fig. 2: The simplified simulation model

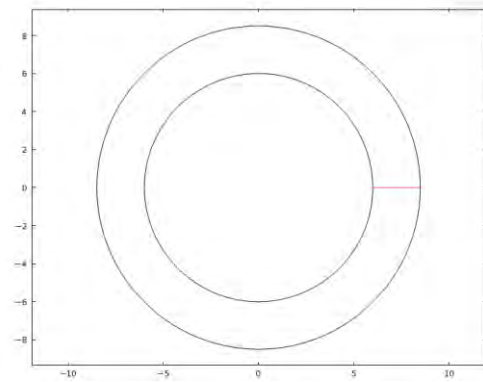


Fig. 3: The evaluation line along the radius of the insulation material

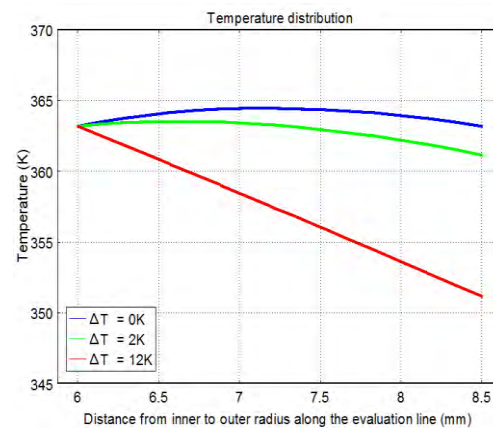


Fig. 4: Temperature distributions for the different ΔT , with $\alpha = 0,094$ and $\beta = 0.1$

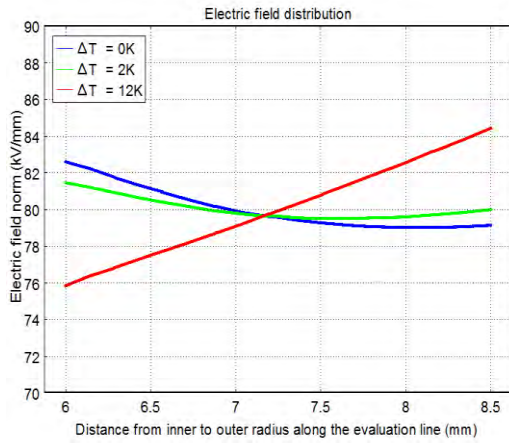


Fig. 5: Electric field distributions for the different ΔT , with $\alpha = 0,094$ and $\beta = 0.1$

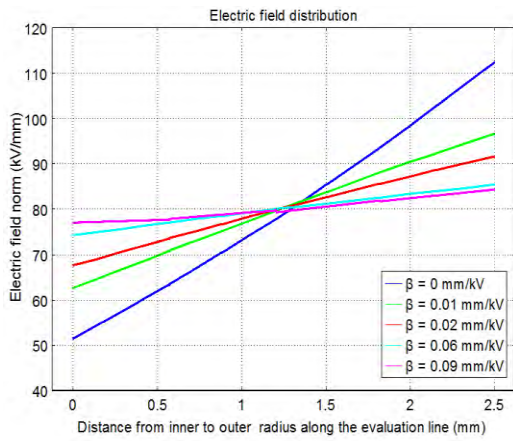


Fig. 6: Electric field distributions for the different β , with $\Delta T = 12K$

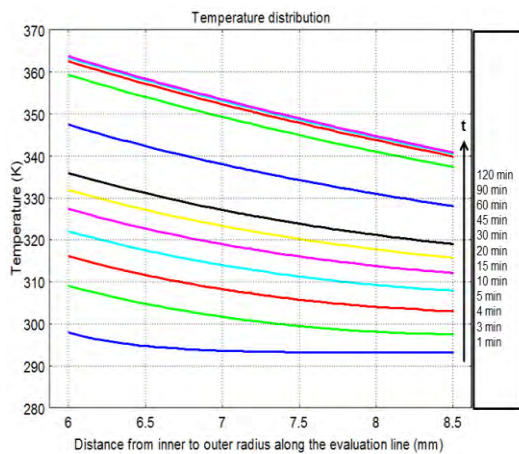


Fig. 7: Temperature distributions during the heating

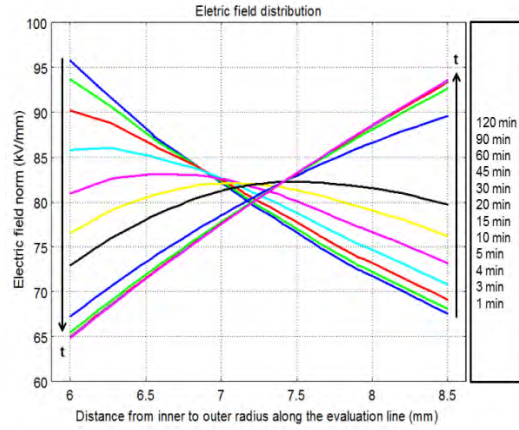


Fig. 8: Electric field distributions during the heating

3.3 Time-dependent Study

In this subsection the simulations for the heating process are described. The electrostatic field distribution of a normal cylindrical capacitor is used as the initial value for the time integrator and a time-dependent solver BDF is selected to solve this problem. A general inward heat flux Q_i is set as the boundary condition at the inner radius. At the outer radius the heat flux is set to an outward heat flux with $Q_{out} = h \cdot (T - T_{ext})$, where T_{ext} is the ambient temperature with 20°C . As in the stationary study, the potential at the inner radius is set to 200kV and the outer radius is grounded. The temperature distribution and electric field distribution during the heating process are shown in Fig. 7 and Fig. 8. With the increasing temperature over time and increasing temperature difference ΔT across the insulation material the field inversion effect occurs.

3.4 A non-rotationally symmetric model

Simulations for an extended non-rotationally symmetric model are also carried out (Fig. 9). With increasing temperature the thermoplastic insulation material, e.g. LDPE (low density Polyethylene), becomes softer and the inner conductor sags because of gravity [13]. For this case the cable is no longer rotationally symmetric. The result for the stationary solution of this model in the cross-section is shown in Fig. 10. It shows that the electric field in lower areas is much larger than in the other areas. The electric field along

the evaluation line 1 with different ΔT is also presented in Fig. 11. Fig. 12 shows the electric field distributions during the heating process for this model. This result is very similar to the results of the heating process for the rotationally symmetric model.

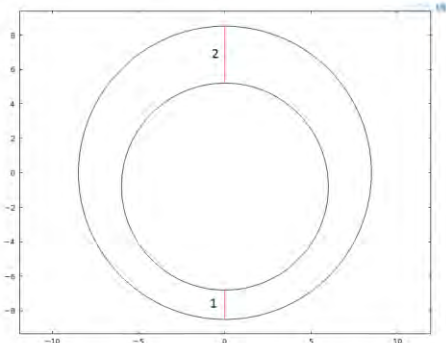


Fig 9: The non-rotationally symmetric model and the 2 evaluation lines (red)

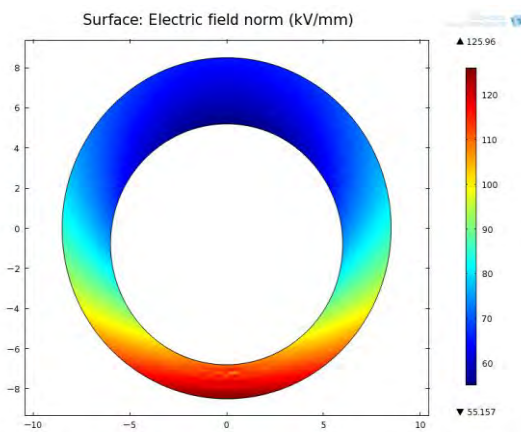


Fig 10: Electric field distribution in The cross-section of the cable

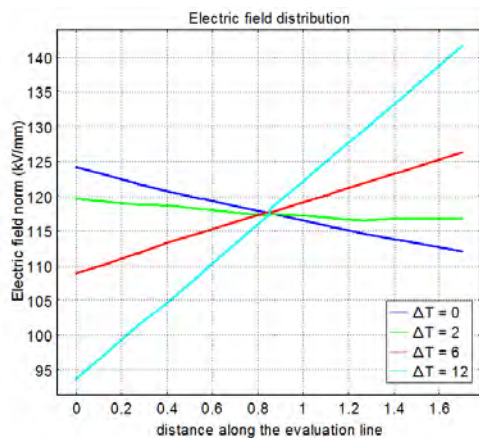


Fig. 11: Electric field distributions along the evaluation line 1 with the different ΔT

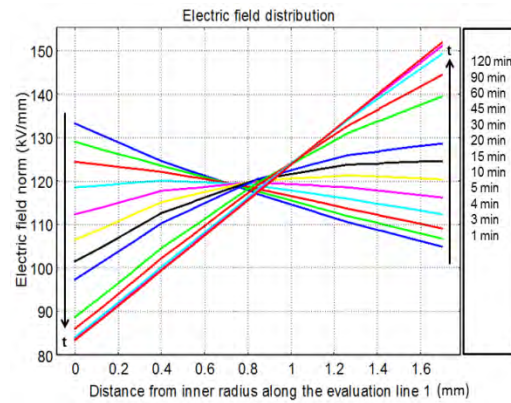


Fig. 12: Electric field distributions along the evaluation line 1 during the heating process

4. Conclusions

For the PE insulated cables both the temperature differences ΔT across the insulation material and the electric field coefficient β have a significant influence on the electric field distribution because PE has a nonlinear electric conductivity which can be approximated as a function of the temperature and the electric field. A phenomenon known as field inversion occurs at higher temperature differences across the insulation material. This can lead to space charge accumulation, which is generally claimed to be one of the main factors for degradation of the insulation material [14]. In [3] ohmic losses were neglected, despite of the nonlinearity of the material properties. Our results show that this assumption is reasonable, at least for the inspected parameters. Our coupled electric-thermal simulation results for a two-dimensional rotationally symmetric model using COMSOL match the results in [3] well. The concordance of theory and numerical simulation indicates that results for more complex models are trustworthy. Therefore, an extended non-rotationally symmetric model has been assembled and simulated for the stationary and the time-dependent problems. For this model the inversion of electric field takes place as well.

5. References

1. Prof. Bärsch, Prof. Kindersberg, Nichtlineare Dielektrische Funktionseigenschaften von Dielektrika, *ETG-Fachbericht zum Workshop "Werkstoffe mit nichtlinearen"*

dielektrischen Eigenschaften", **Vol 10**, VDE Verlag, Berlin, Offenbach, 13.03.08.

2. Jeronse, M., Charges and Discharges in HVDC Cables-In Particular in Mass-Impregnated HVDC Cables, *Doctoral Thesis*, TU Delft, Netherlands, Delft University Press, 1997.

3. Uwe Richert, Ein Beitrag zur Eignung extrudierter Polyethylenisierungen für Gleich-spannungskabel, *diss.*, TU Dresden, 2001.

4. Jiang, GG, Boggs, S., High Field Conductivity of Polyethylene, *10th International Symposium on High Voltage Engineering (ISH'97)*, Montréal, Québec, Canada, August 25-29, 1997.

5. Salah Khalil, M., Gastli, A., Dependence of DC Insulation Resistivity of Polyethylene on Temperature and Electric Field, *1997 IEEE Annual Report*, Conference on Electrical Insulation and Dielectric Phenomena, Minneapolis, Oct. 19-22, 1997, pp. 296-299.

6. Coelho, R., Mirebeau, P., On the Field Distribution in a coaxial DC Power Cable, *REE, Série Spécialisée, Câbles d' énergie et science des isolants*, **Vol 1**, 1996, pp. 96-101.

7. Hampton, R.N., Chang, F., Hobdell, S.B., What Happens to Material under HVDC? *CIGRÉ SESSION 2000*, Panel 2: Effect of Electrical Stresses on Insulating Materials, P2-001.

8. Carslaw, H. S., Jaeger, J. C., Conduction of heat in solids, **Second Edition**. Oxford University Press, 1959.

9. Ern, A., Guermond, J., Theory and Practice of Finite Elements, *Applied Mathematical Sciences*, **Volume 159**, Springer-Verlag New York, 2004.

10. Peschke, E., von Olshausen, R., Kabelanlagen für Hoch- und Höchstspannung, 1998, Publicis-MCD-Verlag, München.

11. Bungay, E.W.G., McAllister, D., Electric Cable Handbook, 1990, Blackwell Science Ltd, Oxford.

12. Salah Khali, M., International Research and Development Trends and Problems of HVDC Cables with Polymeric Insulation, *IEEE Electrical Insulation Magazine*, **Vol 13**, No. 6, 1997, pp. 35-47.

13. Hans J. Mair und 9 Mitautoren, Kunststoffe in der Kabeltechnik: Entwicklung, Prüfung, Erfahrungen, Tendenzen, 3., völlig neubearbeitete und erweiterte Auflage, Renningen-Malmsheim: expert verlag, 1999.

14. D. Fabiani et. Al., Polymeric HVDC Cable Design and Space Charge Accumulation, Part 1: Insulation/Semicon Interface, *IEEE*

Electrical Insulation Magazine, **Vol. 23**, No.6, 2007.